Nitrogen incorporation effects in Fe(001) thin films

J. L. Menéndez,[a] G. Armelles, A. Cebollada, and F. Briones
Instituto de Microelectrónica de Madrid (CNM-CSIC), Isaac Newton 8-PTM, 28760 Tres Cantos, Madrid, Spain

F. Peiró, F. Güell, and A. Cornet
Electronic Materials and Engineering, Facultat de Fisica, Universitat de Barcelona, Avenida Diagonal 645-647, E-08028 Barcelona, Spain

M. L. Fernández Gubieda and J. Gutiérrez
Departamento de Electricidad y Electrónica, Universidad del Pais Vasco, P.O. Box 644, 48080 Bilbao, Spain

C. Meyer
Laboratoire Louis Néel, CNRS, 25 Avenue des Martyrs, BP 166, 38042 Grenoble Cedex 9, France

(Received 11 August 2000; accepted for publication 5 March 2001)

Nitrogen incorporates into Fe thin films during reactively sputtered TiN capping layer deposition. The influence that this nitrogen incorporation has both on the structure and magnetic properties is discussed for a series of Fe(001) thin films grown at different temperatures. A higher nitrogen content is accompanied by distortion in the Fe lattice and by reduction in the Fe magnetization saturation as well as in the effective anisotropy constant, K. The reduction of K brings as a consequence lowering in the coercive field with respect to equivalent Fe films with no nitrogen present. © *2001 American Institute of Physics.* [DOI: 10.1063/1.1368398]

I. INTRODUCTION

It is well known[1–3] that incorporation of nitrogen into the Fe lattice leads to the formation of iron nitrides, such as Fe_2N, ϵ-$Fe_{2-3}N$, γ-austenite, γ'-Fe_4N, α'-martensite, and α''-martensite ($Fe_{16}N_2$). In general, Fe_xN_y systems are interesting from an applied point of view due to the giant magnetic moments reported in the literature[4–6] and the presence of perpendicular magnetic anisotropy[7] found in the $Fe_{16}N_2$ (α'') system.

There have been several approaches to obtain α'' phase in thin film form using different deposition methods such as reactive sputtering deposition below 200 °C plus an annealing process,[8] nitrogen ion implantation,[9] molecular beam epitaxy in a nitrogen ambient,[10] and ion beam assisted deposition plus annealing.[11] In this work, nitrogen is introduced into the Fe lattice through exposure to an $Ar+N_2$ plasma present during the reactive deposition of the TiN capping layer. The questions that are addressed in this work concern how nitrogen enters the Fe layers and the effect it has on fundamental magnetic magnitudes such as saturation magnetization and anisotropy constants. Whether nitrogen incorporates into the Fe lattice or at the grain boundaries conditions interpretation of the observed changes in the physical properties. In the former case, a Fe_xN_{1-x} compound would be present in which the eventual electronic structural changes would be driven by Fe–N orbital hybridization or even the formation of a different Fe–N phase. In the latter case, the system could be regarded as pure Fe with a distorted lattice, and in that case the changes in the electronic structure would be driven by changes in the Fe–Fe interatomic distances of the body-centered-cubic (bcc) lattice.

II. EXPERIMENT

In this work, the properties of a series of 200 Å bcc Fe(001) films grown on MgO(001) will be described. Details of the deposition process can be found in Ref. 12. Relevant aspects are Fe growth temperature, which was varied between room temperature (RT) and 700 °C in steps of 100 °C, and the capping layer used, which was a 15 Å TiN film reactively sputtered at RT (plasma energy 100 V) using a mixture of 70% Ar and 30% N_2, yielding a total pressure of 8×10^{-4} mbar during cap deposition.

In situ structural characterization was done by reflection high-energy electron diffraction (RHEED), while complementary measurements were performed *ex situ* by x-ray diffraction (XRD) and transmission electron microscopy (TEM). The composition of the different films was determined by depth profiling x-ray photoemission spectroscopy (XPS). Finally, determination of saturation magnetization and magnetic anisotropy constants was done by a combination of vibrating sample magnetometry (VSM), superconducting quantum interference device (SQUID), and magneto-optical torque[13] (MOT) measurements.

III. RESULTS AND DISCUSSION

It has been previously found[12] that nitrogen incorporates into the Fe lattice during reactive sputtering deposition of a TiN capping layer. This nitrogen incorporation occurs during the exposure of the Fe surface to an $Ar+N_2$ plasma and it gives rise to expansion in the Fe out-of-plane interplanar distance. For example, structures grown under equivalent ex-

[a]Author to whom correspondence should be addressed; electronic mail: menendez@imm.cnm.csic.es

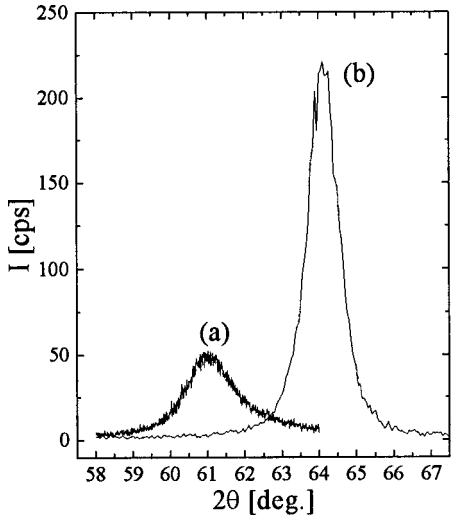

FIG. 1. Symmetric XRD scans for Fe samples grown at RT (a) exposed and (b) not exposed to an $Ar+N_2$ plasma.

perimental conditions but not exposed to an $Ar+N_2$ plasma did not exhibit any relevant lattice distortion. As an example, Fig. 1 shows XRD scans for two equivalent samples grown at RT. The peak around $2\theta=61°$ [Fig. 1(a)] is observed either when the sample is exposed to an $Ar+N_2$ plasma with further deposition of a Pt or Ti capping layer or when a TiN capping layer is grown reactively with the same gas mixture. On the other hand, the peak around the bulk Fe value [Fig. 1(b)] is found when the sample is covered by either a Pt or a Ti capping layer, but never exposed to an $Ar+N_2$ plasma. This clearly shows that nitrogen coming from the reactive plasma leads to the observed distortion. In TiN capped samples, this expansion depends on the Fe layer growth temperature.

As mentioned before, a series of Fe samples, deposited at temperatures ranging from RT to 700 °C, was grown to study the effects that this nitrogen incorporation has on both the structural and magnetic properties. For this series, the well known epitaxial relation Fe[100], (001)//MgO[110], (001) was confirmed both by RHEED and XRD asymmetric phi scans. The RHEED patterns indicate a gradual increase of crystalline quality from RT to 700 °C deposition with sharper, more intense diffraction bars for higher growth temperatures. Quantitative structural characterization obtained from XRD is shown in Fig. 2. Figure 2(a) shows in-plane and out-of-plane lattice parameters experimentally determined by combined symmetric and asymmetric XRD measurements. While in-plane parameters are equal to bulk values within experimental error, two clear regions can be distinguished for the out-of-plane lattice constants. For low growth temperatures (i.e., between RT and 200 °C), the interplanar distances exhibit big expansions, which are between 5.8% for the RT sample and 4.8% for 200 °C growth temperature. At 300 °C the Fe(200) diffraction splits into two peaks, one corresponding to a higher degree of lattice expansion (about 4.3%) and the other to a lower one (1.8%). For 300 °C and higher growth temperatures, the expansion slowly decreases, reaching almost zero for growth at 700 °C. The expansion found in the out-of-plane lattice parameters

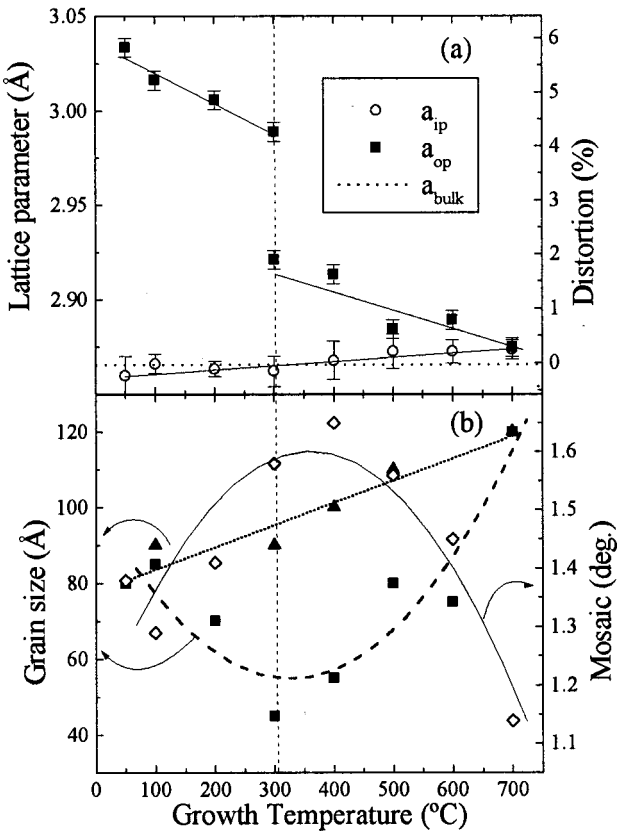

FIG. 2. Structural parameters for several Fe thin films grown at different temperatures: (a) in-plane and out-of-plane lattice parameters (the dotted line corresponds to the bulk value); (b) perpendicular grain size (closed squares) and mosaic spread (open diamonds) for the same set of samples. The values of the grain size for an equivalent series with a Pt capping layer are also indicated (closed triangles).

accompanied by bulk values for the in-plane lattice parameters is an unexpected result if elastic behavior happened. According to elasticity theory, out-of-plane expansion should be accompanied by in-plane contraction. In this system, the free energy in the presence of in-plane biaxial stress, $\sigma_x=\sigma_y\neq 0=\sigma_z$, is given by

$$f=\tfrac{1}{2}c_{11}(2e_{xx}^2+e_{zz}^2)+c_{12}(e_{xx}^2+2e_{xx}e_{zz})-2\sigma_x e_{xx}, \qquad (1)$$

where c_{ij} are the elastic constants. This in-plane biaxial strain leads to a strain tensor, e, of the film with the following form:

$$e=e_0\begin{pmatrix}1&0&0\\0&1&0\\0&0&-2\dfrac{c_{12}}{c_{11}}\end{pmatrix}\approx e_0\begin{pmatrix}1&0&0\\0&1&0\\0&0&-1.2\end{pmatrix}, \qquad (2)$$

where the elastic constants for α-Fe, $c_{11}=2.41\times10^{11}\,\mathrm{N/m^2}$ and $c_{12}=1.46\times10^{11}\,\mathrm{N/m^2}$ have been used. This result implies that, according to the elastic theory, the expansion in the film normal direction should be 20% larger than the in-plane biaxial compression. This indicates that it is more likely the formation of a FeN phase, rather than simply a Fe distortion. The influence of interstitial nitrogen in strain has been studied for Fe–N–Si sputter-deposited films,[14] where it

was also explained to be the cause for a nonelastic component of the strain. N incorporates into the Fe lattice as an interstitial during reactive (Ar+N) plasma exposure along TiN growth and causes tetragonal lattice distortion of the bcc lattice in the perpendicular or growth direction only, since in the (001) plane the film is anchored to the substrate and is not able to expand.

This transition temperature of 300 °C also manifests itself in other measured structural parameters, such as the perpendicular grain size [estimated from the Fe(200) peak breadth using Scherrer's formula] and mosaic spread. Figure 2(b) shows the dependence of these two parameters with respect to the Fe growth temperature. The generally assumed behavior in thin film growth is that higher growth temperatures give rise to structures with both higher grain size and interface coherence with the substrate, with this second effect producing a reduction in mosaic spread. Regarding the grain size of the structures presented in this work, values of around 80 Å are measured for RT and 100 °C growth temperatures, diminishing while increasing the growth temperature and reaching a minimum of 45 Å at 300 °C. The grain size then increases continuously with growth temperature, reaching a maximum value of 120 Å for 700 °C. In parallel, mosaic spread exhibits similar behavior, with minimum values (higher crystalline quality) for low and high growth temperatures, while higher mosaicity is obtained for intermediate growth temperatures (1.65° for 400 °C). The behavior found here clearly does not follow the general rule previously described and besides it is, in principle, in contradiction with the findings of a gradual increase of crystalline quality with growth temperature by *in situ* RHEED pattern inspection. To understand this apparent contradiction, it should be kept in mind that the incorporation of nitrogen into the Fe lattice takes place after deposition of Fe and cool down to RT. A series of samples with a capping of Pt and no exposure to N plasma was grown under equivalent conditions to the ones with a capping of TiN. In this case, both the in-plane and out-of-plane Fe lattice parameters are close to the bulk value, independent of the growth temperature. The Fe crystalline quality (grain size) monotonously increases with increasing Fe deposition temperature, ranging from 90 to 120 Å. These results are shown in Fig. 2(b) for comparison with those obtained for nitrided structures.

In the series with a TiN capping and deposition temperatures above 400 °C, the Fe films are highly compact and the incorporation of nitrogen is low, the distortion and the crystalline quality being almost unaffected. For deposition temperatures below 300 °C, the Fe films are highly porous and the incorporation of nitrogen is homogeneous, leading to a high and homogeneous distortion. Because the nitridation is homogeneous, the crystalline quality is not largely decreased. However, for 300 and 400 °C deposition temperatures the incorporation of nitrogen is not homogeneous and leads to two phases with different distortions. In this case, the width of the XRD peaks is given by the fluctuations of the local lattice parameter, i.e., the dimensions of the regions with uniform distortion or a coherent lattice.

Additional structural information can be extracted from TEM experiments performed on a TiN capped Fe film grown

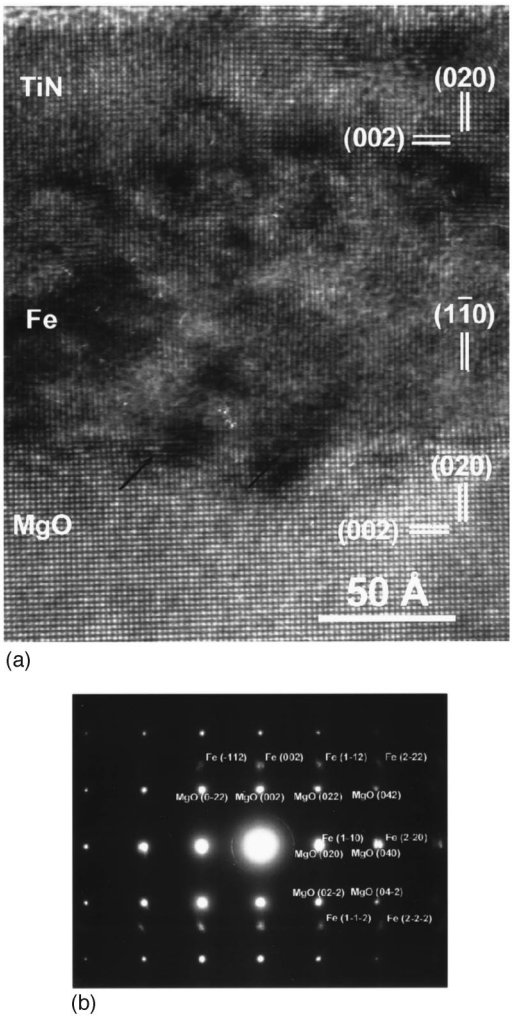

FIG. 3. TEM results for the Fe thin film grown at RT. (a) Diffraction pattern of the Fe–MgO interface region, obtained along the $[100]_{MgO}$ and $[110]_{Fe}$ zone axes. (b) Cross-sectional HRTEM micrograph of the whole structure with the orientation relationship TiN(001)[100]//Fe(001)[110]//MgO(001)[100]. The arrows denote the presence of dislocations at the interface between Fe and MgO.

at RT exhibiting large distortion from XRD characterization. According to indexation of the spots in the selected area diffraction pattern of Fig. 3(a), the Fe adopts a bcc structure with an orientation relationship MgO(001)[100]// Fe(001)[110], in agreement with RHEED and XRD observations. According to the bulk values $a_{MgO}=4.21$ Å and $a_{Fe}=2.87$ Å, and taking into account the fact that the planes perpendicular to the interface are the $(020)_{MgO}$ and $(1\text{-}10)_{Fe}$ planes, the corresponding nominal lattice mismatch is 3.7%. As explained above, elasticity theory would conclude a reduction of the lattice parameter of Fe along the growth direction if Fe had remained under tension on the MgO substrate. The measurements of the lattice parameter from the diffraction pattern of different samples grown at room temperature yield values for a_{Fe} around 2.98 Å along the grown direction, which is higher than the expected theoretical value if the Fe were completely relaxed on the MgO. This higher lattice parameter with respect to the bulk value indicates an expansion of the Fe in the growth direction of 3.8%, in agreement with the XRD results.

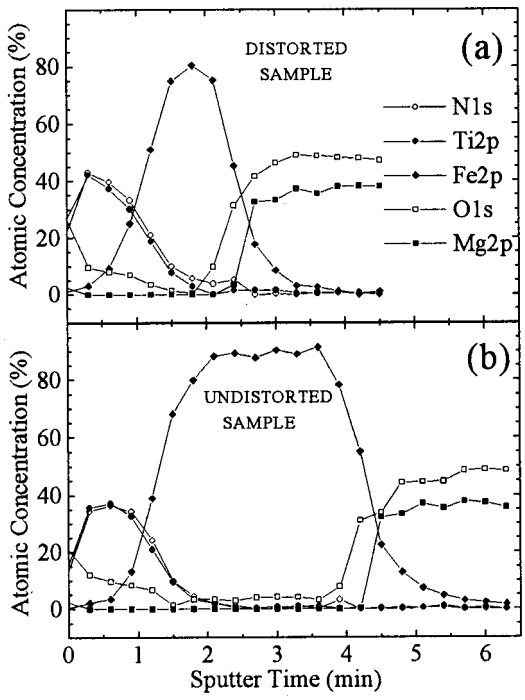

FIG. 4. XPS depth profiling for (a) distorted and (b) undistorted samples.

Figure 3(b) presents a high resolution transmission electron microscopy (HRTEM) image of the same sample. Otherwise, the Fe structure is quite homogeneous, with no evidence of possible different FeN phases coexisting. The arrows indicate the presence of dislocations at the interface between the Fe and the MgO, allowing the Fe layer to relax. The interfaces of Fe with TiN and MgO are very rough and can be distinguished because of the contrast extinction of planes $(002)_{Fe}$ whose interplanar distance ($d_{(002)Fe}=1.43$ Å) is at the limit of the point resolution of the microscope. Conversely, the $(002)_{MgO}$, $(020)_{MgO}$, and $(110)_{Fe}$ planes ($d_{(020)MgO}=2.1$ Å; $d_{(1\text{-}10)Fe}=2.02$ Å) are clearly resolved.

Once the presence of nitrogen in the Fe lattice is clearly concluded, the next important question concerns the amount of N in the Fe layer and whether it is distributed homogeneously along the thickness of the film. In order to clarify this point, XPS depth profiling experiments have been performed in both distorted and undistorted samples, therefore with higher and lower nitrogen contents, respectively, with the results displayed in Fig. 4 for representative peaks. For this specific experiment the thickness of the film with the highest lattice distortion (100 Å) is lower than the thickness of the rest of the samples studied in this work (200 Å). No difference in the distortion for 100 or 200 Å films grown under the same conditions has been found, therefore a thickness dependent strain can be ruled out. In both samples, the Ti and N signals from the capping layer fall when the Fe signal starts to increase. They coexist during a wide range in depth due to interface roughness, as observed by TEM [Fig. 3(b)], as well as to Ti and N implantation during the sputtering etching process. The same effects hold for the Fe–MgO interface. Regarding the nitrogen concentration in the Fe layer, there are small differences between the distorted and the undistorted samples. While in the undistorted sample the atomic concentrations of nitrogen and titanium are equal, in the distorted sample the amount of nitrogen is always more than the amount of titanium. This extra amount of nitrogen in the distorted sample is present before the sputtering etching process and is responsible for the observed lattice distortion. A rough estimation of the extra amount of nitrogen in the sample with the highest lattice distortion from the depth profiling experiments leads to a 2% which is close to the resolution of the technique. Vegard's law is another way of estimating the amount of nitrogen in the distorted films. In this case, considering the lattice parameters for Fe and $Fe_{16}N_2$, the expected amount of Fe for the film with the highest distortion should be around 5%. These values give an idea of the error bar in the determination of the actual nitrogen content.

The next question that arises is the possible effect that nitrogen incorporation can produce in the magnetic properties of Fe. As mentioned in Sec. I, the Fe–N system has been thoroughly studied by the observation of giant magnetic moments connected to martensite structure formation.[15] On the other hand, and taking into account the positive magnetostriction constant of Fe along the (100) direction (21×10^{-6}),[16] another effect that this vertical expansion would produce is the appearance of perpendicular magnetic anisotropy. The magnetic properties of these series of samples have been studied by a combined use of VSM and SQUID, for the determination of the hysteresis loops and Ms values, and MOT for the quantification of the magnetic anisotropy constants.

The hysteresis loops have been measured with the field applied along three directions: two in plane along the [001] and [011] Fe crystalline directions and one out of plane along the (001) direction. Despite the positive magnetostriction value of Fe and the out-of-plane lattice expansion, no indication of perpendicular magnetic anisotropy was detected even for the most distorted sample. In Fig. 5(a) the values of Ms for selected samples are shown. Measurements were carried out at 10 K. To eliminate any kind of spurious (diamagnetic or paramagnetic) contribution from the substrate or capping layer, a 15 Å TiN(001) film was deposited on an equivalent MgO(001) substrate to be used as a reference sample, with the contribution from the substrate and capping layer subtracted. The error bars for the magnetization value mainly come from determination of the thickness. Other factors such as data treatment due to subtraction of the contribution of the capping layer or the set-up error were found to be negligible with respect to the thickness determination error. Since the unit cell volume is different from that corresponding to the bulk due to distortion, the saturation moment shown in Fig. 5(a) was corrected for volume effects. The resulting saturation magnetization shows a decrease with increasing distortion: Samples with high distortion, those grown below 300 °C, have their saturation magnetization reduced up to 15%. The sample grown at 300 °C has larger saturation magnetization, showing a decrease of 7% with respect to the bulk value. Finally, when the distortion is low, above 300 °C, the saturation magnetization of the films is close to the Fe bulk value within experimental error. Taking

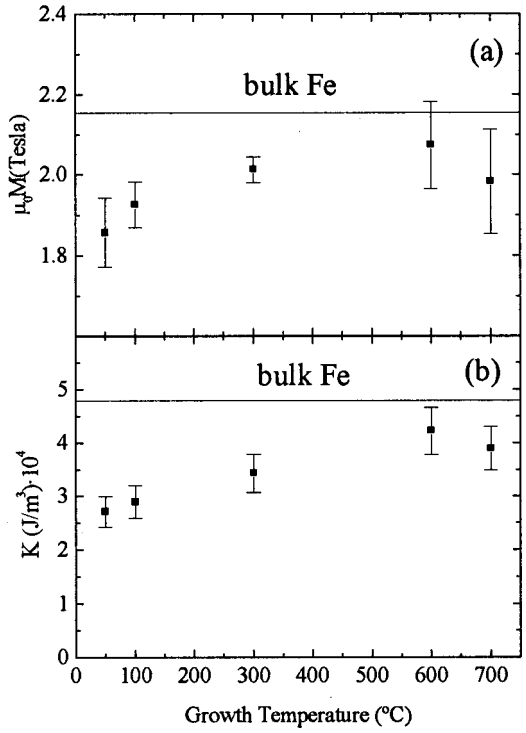

FIG. 5. (a) Saturation magnetization and (b) anisotropy constant for samples grown at different temperatures.

into account the fact that distortion is related to the amount of nitrogen entering the sample as discussed above, the decrease observed in the saturation magnetization can be directly related to hybridization effects between the nitrogen and the Fe atoms in the Fe layer. Compared with the results reported in the literature,[15,17] this decrease in the saturation magnetization is not surprising. For example, whenever the α''-$Fe_{16}N_2$ structure is altered, either through stoichiometry or through chemical disorder of the N atoms in the $Fe_{16}N_2$ structure, the saturation magnetization is reduced, below even the bulk Fe value. In the Fe films reported in this work, nitrogen incorporates into the Fe lattice from the reactive plasma during deposition of the capping layer and no chemical order is obtained. In the present films several effects are expected to contribute: on one hand, an increase in the magnetic moment due to the lattice expansion,[18] on the other hand, a reduction in the magnetic moment through Fe–N hybridization in a chemically disordered structure.[17] Since a reduction in the magnetic moment of this series of films is observed, hybridization effects are concluded to be dominant.

With regard to the experimentally determined in-plane effective magnetic anisotropy constant, K [Fig. 5(b)], it exhibits the same dependence with growth temperature as Ms. Values close to the magnetocrystalline anisotropy constant for bulk Fe are found in films grown at high temperatures. At low growth temperatures there is a continuous reduction in K of up to 46% for the RT sample with respect to the magnetocrystalline anisotropy constant for bulk Fe, that is, much larger than the reduction observed in Ms for the same sample. Nitrogen incorporation is one of the reasons for this reduction since it leads to the mentioned Fe–N hybridization. As mentioned in Ref. 19, the dominant contribution to the magnetic anisotropy in the RT sample comes from the magnetocrystalline term. Therefore, any effect on the magnetocrystalline term will affect the effective magnetic anisotropy constant. Since the crystalline anisotropy is due mainly to spin–orbit coupling and it can be reduced by nitrogen incorporation via Fe–N hybridization, it is reasonable to attribute the observed reduction in K to the nitrogen in the Fe layer. Other factors that do not affect Ms but that can modify the experimentally measured effective magnetic anisotropy constant are of morphological nature, such as grain size and interface roughness. Nevertheless, quantification of these factors is difficult to achieve with the information available. Another relevant parameter, especially in order to determine the phase of the FeN, is the coercive field. In these films, the coercive field increases with increasing deposition temperature (not shown here), but the same effect was observed in an equivalent series grown without N, which indicates that the evolution is related more to the morphology than to the FeN phases that could have been formed.

IV. CONCLUSIONS

Growth of TiN by reactive sputtering on Fe produces high distortion on the out-of-plane interplanar distances of up to 6% for Fe films grown at RT as observed by TEM and XRD due to inclusion of nitrogen in the Fe layer. The amount of nitrogen in the most distorted sample is estimated to be 2% according to XPS. With regard to the magnetic properties, no perpendicular anisotropy has been found despite the positive magnetostriction and it has been shown that nitrogen incorporation into the Fe lattice induces a reduction both in Ms and in K. In both cases, this reduction is due to Fe–N orbital hybridization.

ACKNOWLEDGMENTS

This work was carried out under the financial support of the Spanish Commission of Science and Technology (CICyT) and Comunidad Autónoma de Madrid. One of the authors (J.L.M.) wants to acknowledge Comunidad de Madrid and its Consejería de Educación y Cultura for financial support. The authors would like to acknowledge E. Snoeck of CNRS for his advice about TEM sample preparation and C. Boubeta for the series with Pt deposited.

[1] K. H. Jack, Proc. R. Soc. London, Ser. A **208**, 216 (1951).
[2] W. B. Pearson, *A Handbook of Lattice Spacings and Structures of Metals and Alloys* (MacMillan, New York, 1948).
[3] J. D. Fast and M. B. Verrijp, J. Iron Steel Inst., London **180**, 337 (1955).
[4] T. K. Kim and M. Takahashi, Appl. Phys. Lett. **20**, 492 (1972).
[5] M. Komuro, Y. Kozono, M. Hanazono, and Y. Sugita, J. Appl. Phys. **67**, 5126 (1990).
[6] Y. Sugita, K. Mitsuoka, M. Komuro, Y. Kozono, and M. Hanazono, J. Appl. Phys. **70**, 5977 (1991).
[7] H. Takahashi, M. Igarashi, A. Kaneko, H. Miyajima, and A. Sugita, IEEE Trans. Magn. **35**, 2982 (1999).
[8] M. Takahashi, H. Shoji, H. Takahashi, H. Nashi, T. Wakiyama, M. Doi, and M. Matsui, J. Appl. Phys. **76**, 6642 (1994).
[9] K. Nakajima and S. Okamoto, Appl. Phys. Lett. **54**, 2536 (1989).

[10] Y. Sugita, H. Takahashi, M. Komuro, K. Mitsuoka, and A. Sakuma, J. Appl. Phys. **76**, 6637 (1994).
[11] Z.-Y. Zao, H. Jiang, Z.-K. Liu, D.-D. Huang, F.-G. Qin, S.-C. Zhu, and Y.-X Sun, J. Magn. Magn. Mater. **177–181**, 1291 (1998).
[12] J. L. Menéndez, G. Armelles, A. Cebollada, A. Delin, and D. Weller, Phys. Rev. B **62**, 10498 (2000).
[13] G. Armelles, J. L. Costa-Krämer, J. I. Martín, J. V. Anguita, and J. L. Vicent, Appl. Phys. Lett. **77**, 2039 (2000).
[14] K. Uchiyama and R. C. O'Handley, IEEE Trans. Magn. **35**, 2024 (1999).
[15] M. Takahashi and H. Shoji, J. Magn. Magn. Mater. **208**, 145 (2000), and references therein.
[16] B. D. Cullity, in *Introduction to Magnetic Materials*, edited by B. D. Cullity (Addison–Wesley, Reading, MA, 1972).
[17] J. M. D. Coey and P. A. I. Smith, J. Magn. Magn. Mater. **200**, 405 (1999), and references therein.
[18] V. L. Moruzzi and P. M. Marcus, J. Appl. Phys. **64**, 5598 (1988).
[19] J. L. Costa-Krämer, J. L. Menéndez, A. Cebollada, F. Briones, D. García, and A. Hernando, J. Magn. Magn. Mater. **210**, 341 (2000).